UC San Diego
UC San Diego Previously Published Works

Title

Endogenous Intracellular Cathelicidin Enhances TLR9 Activation in Dendritic Cells and Macrophages

Authors

Nakagawa, Yukinobu
Gallo, Richard L

Endogenous intracellular cathelicidin enhances TLR9 activation in dendritic cells and macrophages[*]

Yukinobu Nakagawa and **Richard L. Gallo**[*]

Division of Dermatology, University of California, San Diego, CA

Abstract

Cathelicidins are a gene family best known for their antimicrobial action, but the diverse mature peptides they encode also have other host defense functions. The human cathelicidin peptide LL-37 enhances recognition of nucleic acids, an action whose significance is seen in human diseases such as psoriasis where it is associated with increased type-1 interferon production. This function has been attributed to the extracellular action of the peptide to facilitate uptake of nucleic acids. Here, we demonstrate that the murine mature cathelicidin peptide (CRAMP), encoded by the mouse gene (*Camp*), is functionally distinct from the human mature peptide (LL-37), as it does not facilitate CpG entry. However, mouse cathelicidin does influence recognition of CpG as bone marrow-derived dendritic cells (BMDCs) from $Camp^{-/-}$ mice have impaired CpG responses and $Camp^{-/-}$ mice had impaired response to CpG given intravenously or subcutaneously. We show that cathelicidin concentrates in Lamp1 positive compartments, is colocalized with CpG in the endolysosome, can be immunoprecipitated with TLR9, and binds to CpG intracellulary. Collectively, these results indicate that the functions of cathelicidin in control of TLR9 activation may include both intracellular and extracellular effects.

Introduction

Recognition of microbial pathogens is an essential element for host defense (1, 2). Toll-like receptors (TLRs) are family of pattern recognition receptors that play a central role in the initiation of immune responses against a number of pathogens and also served to recognize a wide range of molecules released after injury that collectively have been referred to as Damage Associated Molecular Patterns (DAMPs) (3, 4). TLR9 is a key receptor for the recognition of DNA, and frequently studied by its response to synthetic CpG-DNA (CpG) to mimic DNA found more abundantly in microbes (5). TLR9 exits in the endoplasmic reticulum (ER) and upon stimulation with CpG, it relocates to the endolysosomal compartments where TLR9 binds to CpG after undergoing proteolytic cleavage by asparagine endopeptidase and cathepsins (6–9). After CpG binding, TLR9 signaling is initiated by recruitment of the adaptor molecule, MyD88 and subsequent phosphorylation of MAPKs and activation of NF-kB, leading to production of proinflammatory cytokines (1, 10). In plasmacytoid DCs (pDCs), CpG-TLR9 complexes are transported to lysosome-related organelles (LROs) where MyD88-dependent IRF7 activation is initiated, leading to

IFN-α production (11, 12). Previous reports have shown that TLR9 responses are enhanced by accessory molecules such as HMGB1, granulin and LL-37 (13–17). In particular, the capacity of the cathelicidin peptide LL-37 to bind to DNA has been shown to facilitate delivery into endosomes and activation of TLR9, thus breaking self-tolerance to endogenous mammalian DNA released upon cell lysis during injury.

The capacity of the cathelicidin LL-37 to influence TLR9 function is consistent with the broad host defense functions that have been associated with this family of peptides. Cathelicidins are one gene family within the highly diverse group of antimicrobial peptides and proteins that collectively have been referred to as AMPs (18, 19). The human and mouse cathelicidin peptides, LL-37 and CRAMP respectively, have been directly shown to play a crucial role in host defense against a wide range of pathogens (20–24). Their essential role in mammalian host defense is likely due to both their broad-spectrum antimicrobial functions and their additional immunomodulatory functions. These immunomodulatory functions appear to depend on the hydrophobicity, charge, and capacity of the mature peptide to either bind ligands or directly activate membrane bound signaling receptors (25–30). For example, LL-37 and CRAMP show affinity for nucleic acids such as DNA and RNA (17, 31–35). LL-37 can aggregate with nucleic acids and protect them from degradation. LL-37 can also deliver DNA or RNA complexes into human pDCs or human myeloid dendritic cells (mDCs), leading to TLR9 or TLR7 activation (17, 31). Cathelicidins can also have an anti-inflammatory role by neutralizing LPS and blocking activation of TLR4 (28, 29). Thus, cathelicidins such as CRAMP and LL-37 influence host defense responses through multiple mechanisms, but all of these observations have focused on the activity of the mature, secreted peptide.

Confirmation of the physiological relevance of cathelicidin has come from several studies of the effects of expression of the gene for CRAMP (*Camp)* in mice. These studies have demonstrated that deletion of *Camp* results in a change in both infectious and inflammatory responses of the skin, lung and gut (20, 21, 23). These phenotypes have also correlated well with human diseases in which cathelicidin is overexpressed or underexpressed (17, 36, 37). However, these observations *in vivo* correlate the observed effects with altered expression of the full-length endogenous cathelicidin precursor protein as well as the mature secreted peptide. Thus, in contrast to many studies of the mature cathelicidin peptide, the function of the endogenous cathelicidin protein under physiological conditions is not well understood. This question may be particularly important as it is the mature cathelicidin domain that is evolutionarily conserved, not the mature peptide.

In this study, we observed that the endogenous expression of cathelicidin is required for normal TLR9 signaling in mice, a finding consistent with observations with the mature human cathelicidin peptide LL-37. However, the mouse peptide CRAMP does not function similarly to LL-37. In contrast, CRAMP was shown to bind to TLR9 and colocalize with CpG in endolysosome without affecting CpG entry in dendritic cells and macrophages. These findings suggest that the endogenous expression of cathelicidin may be a previously unknown intracellular accessory molecule for TLR9 signaling.

Materials and Methods

Mice and cell lines

C57BL/6 mice were purchased from Jackson Laboratories. $Camp^{-/-}$ mice on C57BL/6 background or Balb/c background were generated in our laboratory as previously described (20). Mice were backcrossed onto C57BL/6 mice for 8 generations or Balb/c mice for 7 generations. All mice were bred in specific pathogen-free conditions. All animal experiments were approved by UCSD's institutional animal care and use committees and were conducted in accordance with the guideline for the care and use of laboratory animals. The mouse keratinocyte cell line Pam 212 and mouse macrophage cell line RAW264.7 was used for Q-PCR experiments.

Reagents and Abs

Anti-CD11c (N418), MHC class II (I-A) (NIMR-4), anti-CD40 (HM40-3), Anti-CD80 (16-10A1), Anti-CD86 (GL1) and anti-mTLR9 (M9.D6) were obtained from eBioscience. Anti-β-actin (AC-74) and thioglycolate were from Sigma-Aldrich. Anti-p44/42 MAPK (4695), anti-phospho-p44/42 MAPK (9101), anti-p38 MAPK (9212), anti-phospho-p38 MAPK (9216), anti-IkB-α (9242), anti-phospho-IkBα (2859), anti-SAPK/JNK (9258), anti-HA (2367 and 3724) and anti-phospho-SAPK/JNK (9255) were from Cell Signaling Technology. Anti-EEA1 was from Thermo Fisher Scientific. Anti-LAMP1 (1D4B) was from abcam. Alexa Fluor488 Donkey anti-mouse IgG, Alexa Fluor488 Donkey anti-rat IgG and Alexa Fluor568 Donkey anti-rabbit IgG were from life technologies. Affinity-purified rabbit polyclonal anti-CRAMP Ab which recognizes CRAMP peptide domain was previously generated in our laboratory(38). ODN 1585, ODN 1668, ODN M362, ODN 1668-FITC, ODN M362-FITC, R848, Poly(I:C) HMW, Pam3CSK4, Zymozan, LPS-EB, pUNO-mTLR9-HA and pSELECT-puro-mcs were from invivogen. DOTAP liposomal transfection reagent (DOTAP) was from Roche applied science. Recombinant mouse CRAMP peptide (mCRAMP) was synthesized by Genemed Synthesis Inc.

Quantitative real-time PCR

RNA was isolated using Trizol (Life Technologies). RNA was reverse transcribed using iScript (Bio-Rad). Predesigned Taqman probes and primers were used to quantify *Il6*, *Tnf*, *Il12a* and *Camp* mRNA using Taqman Gene Expression Master Mix and a 7300 Real Time PCR System (Life Technologies) according to manufacturer's instructions. Custom Taqman Probes (Life Technologies) were used for *Gapdh* mRNA quantification. Fold change normalized to host cell *Gapdh* levels relative to the control was calculated using the 2(− Ct) method.

Cell purification

To prepare Flt3ligand (Flt3L)-induced bone marrow-derived DCs (BMDCs), BM cells were cultured for 7 days with 100 ng/ml human Flt3L (PeproTech) in RPMI-1640 medium supplemented with 10% (vol/vol) FBS (Thermo Fisher Scientific), 50 μM 2-ME, 100 U/ml of penicillin and 100 μg/ml of streptomycin (VWR). For purification of Flt3L-induced plasmacytoid DCs (Flt3L pDCs), cells from Flt3L cultures were incubated with anti-B220

MACS beads and positively separated with MACS sorting (MACS separation column, Miltenyi Biotec). The resulting purity was >95% for each experiment. Cells in the negative fraction were used as Flt3L-induced conventional DCs (Flt3L cDCs). GM-CSF-induced BMDCs (GM-CSF BMDCs) were generated from BM cells by culturing cells with GM-CSF (20 ng/ml) in complete RPMI as previously described (39). For thioglycollate-elicited peritoneal macrophage isolation, age and sex-matched WT and *Camp*$^{-/-}$ mice were injected intraperitoneally (i.p.) with 3% thioglycollate. After 72 h, peritoneal macrophages were collected by peritoneal lavage and were plated onto 96-well plates in DMEM (Lonza) supplemented with 10% (vol/vol) FBS, 2 mM L-glutamine and 100 U/ml of penicillin and 100 μg/ml of streptomycin and rested for 24 h.

Plasmids and transfection

DNA encoding full-length CRAMP (amino acids 1–172, mCAP18) or CRAMP peptide (amino acids 140–172) with signal peptide (amino acids 1–27) was synthesized using PCRs and ligated into pSELECT-puro-mcs. Transfection was performed using Fugene HD (Roche) according to the manufacturer's instructions. Cells were used for the experiments 48 h after transfection. RAW264.7 cell clone stably overexpressing pUNO-mTLR9-HA (RAW-TLR9-HA cells) was selected in 4 μg/ml blasticidin and then confirmed the TLR9-HA expression by Western blotting.

ELISA

TNF-α, IL-6 and IL-12p40 concentration was determined using an OptEIA ELISA Set (BD Biosciences). IFN-α was measured by mouse IFN alpha platinum ELISA (eBioscience). IFN-β was measured by mouse IFN beta ELISA KIT (PBL Assay science).

Western blot analysis

For detection of MAPK and IkBα, BMDCs (2×10^6 cells) were starved in RPMI without FCS for 24 h in 12 well. After CpG-B (1 μM) stimulation, protein was isolated by lysing cells in RIPA buffer containing protease inhibitors (Roche) and 1 mM sodium orthovanadate (Sigma-Aldrich). Equal volumes of total cell lysates from WT and *Camp*$^{-/-}$ BMDCs (1×10^5 cells/lane) were loaded on a 4–20% agarose gel and transferred to a PVDF membrane (Bio-Rad). The membranes were immunoblotted with indicated Abs, according to the manufacturer's instructions. β-actin was detected using the mouse monoclonal antibody (1:10,000). For detection of CRAMP, BMDCs were lysed in RIPA buffer containing protease inhibitors. Equal volumes of total cell lysates from WT and *Camp*$^{-/-}$ BMDCs (1×10^6 cells/lane) were used. For detection of secreted CRAMP protein in the culture medium, BMDCs (3×10^7 cells/ml) were cultured and the supernatant was collected at the indicated time. Equal volumes of supernatant (20 μl/lane) were used. CRAMP protein was detected using the rabbit polyclonal CRAMP Ab (1:5000). 680nm and 800nm IR-Dye conjugated secondary antibodies (1:10,000) and an Odyssey imager (LI-COR Biosciences) were used for 2-color Western blotting to analyze both proteins on the same blot. For overexpression experiments, RAW-TLR9-HA cells were transfected with mCAP18 plasmid or control plasmid for 48 h. Cell lysates were immunoblotted with anti-HA Ab, or anti-CRAMP Ab. For TLR9-CRAMP binding assay, RAW-TLR9-HA cells were transfected

with mCAP18 plasmid (mCAP18), CRAMP peptide plasmid (CRAMP) or control plasmid (control). Cells were stimulated with or without 1 μM CpG-C for 90 min and then washed. Cells were lysed with IP lysis buffer (Pierce) and cell lysates were immunoprecipitated with anti-CRAMP or anti-HA and blotted with anti-HA or anti-CRAMP, respectively. For CRAMP-CpG binding assay, 10 μM mCRAMP in PBS was mixed with 1 μM CpG-C or 1 μM biotinylated-CpG-A, -CpG-B or -CpG-C for 1 h at 37°C and then incubated with streptavidin beads (Dynabeads MyOne, life technologies) for 15 min on ice. Streptavidin beads were washed five times using DynaMag (Spin Magnet, life technologies). Biotinylated-CpG-bound mCRAMP was eluted and immunoblotted with anti-CRAMP Ab. In another experiment, 1 μM CpG-C or 1 μM biotinylated-CpG-C and various concentration of mCRAMP were used. In some experiments, WT and *Camp*$^{-/-}$ GM-CSF BMDCs were stimulated with CpG-C or CpG-C-biotin for 1 h and then washed and lysed. Cell lysates were incubated with streptavidin beads and biotinylated-CpG-bound CRAMP was detected with anti-CRAMP Ab.

Flow cytometry

For staining of TLR9, the cells were fixed and permeabilized using a fixation/permeabilization kit (eBioscience). To evaluate surface expression levels of MHC II and co-stimulatory molecules, WT and *Camp*$^{-/-}$ GM-CSF BMDCs were cultured in GM-CSF-containing medium or stimulated with 500 ng/ml LPS overnight and stained with indicated markers. Data were acquired on a BD FACSCanto II flow cytometer (BD Bioscience).

CpG uptake experiments

For the CpG uptake assay, WT and *Camp*$^{-/-}$ GM-CSF BMDCs were cultured with 1 μM FITC-labelled CpG-C in the presence or absence of 10 μM mCRAMP for 1 h, then washed three times and analyzed by flow cytometry. For a microscopy experiment, WT and *Camp*$^{-/-}$ GM-CSF BMDCs were seeded into chamberslides and cultured for 1 h, and then stimulated with 1 μM FITC-labelled CpG-C for 1 h. Cells were washed three times and examined by an Olympus BX41 fluorescent microscope (Scientific Instrument Co.).

In vitro stimulation assays

WT and *Camp*$^{-/-}$ GM-CSF BMDCs (5×10^4 cells/well) were stimulated in 96-well plates with 1 μg/ml Pam3CSK4, 10 μg/ml zymosan, 10 μg/ml Poly(IC), 500 ng/ml LPS, 0.2 μg/ml R848 and various concentration of CpG 1558 (0.3 and 1 μM), CpG 1668 (0.01, 0.1 and 1 μM) and CpG M362 (0.2 and 1 μM) for 15 h. In some experiments, WT and *Camp*$^{-/-}$ GM-CSF BMDCs were stimulated with CpG-C (0.2 μM) in the presence or absence of various concentration of mCRAMP. FLT3L pDCs were stimulated with 0.2 μg/ml R848, 1 μM CpG 1558 and 1 μM CpG M362 for 15 h. FLT3L cDCs were stimulated with 500 ng/ml LPS and 1 μM CpG M362 for 15 h. Thioglycollate-elicited peritoneal macrophages from WT and *Camp*$^{-/-}$ mice were stimulated with 500 ng/ml LPS and CpG M362 (1 μM) for 15 h. In Figure 6C, WT and *Camp*$^{-/-}$ GM-CSF BMDCs were cultured with FITC-labelled CpG-C for 1 h and washed three times, and then seeded onto a 96-well plate and cultured for 15 h. In the experiments using DOTAP, WT and *Camp*$^{-/-}$ GM-CSF BMDCs were stimulated with various concentration of CpG-C or CpG-C/DOTAP complex for 15 h. DOTAP was

used according to the manufacturer's instructions. Briefly, 5 μg of CpG-C in 40 μl of OPTI-MEM (Life Technologies) was combined with 20 μg of DOTAP in 40 μl of OPTI-MEM. After 15 min of incubation, the mixture was diluted with 525 μl of complete RPMI to make 1 μM CpG-C/DOTAP complex. To stimulate BMDCs in the exchanged medium, the conditioned medium from WT and *Camp*−/− GM-CSF BMDCs cultured for 24 h in complete medium was collected and centrifuged to remove debris. WT and *Camp*−/− BMDCs in each medium were stimulated with CpG-C (1 μM) and R848 (0.2 μg/ml) for 15 h. RAW264.7-TLR9-HA cells were transfected with mCAP18 plasmid or control plasmid. Same numbers of cells were seeded on 96 well 48 h after transfection and stimulated with CpG-C (0.2 μM) and LPS (500 ng/ml) for 15 h.

Immunohistochemistry

WT and *Camp*−/− FLT3L cDCs were seeded into chamber slides coated with 5 μg/ml fibronectin (Sigma-Aldrich) for 2 h. Cells were cultured with or without 1 μM CpG-B or FITC-labelled CpG-B for 90 min. Cells were washed, fixed with 4% formaldehyde in PBS for 15 min, and blocked with 3% BSA in PBS. Cells were then stained with anti-EEA-1 Ab or anti-LAMP1 Ab and anti-CRAMP Ab, followed by Alexa Fluor488 Donkey anti-mouse IgG or Alexa Fluor488 Donkey anti-rat IgG and Alexa Fluor568 Donkey anti-rabbit IgG, respectively. Cells were then stained with DAPI (ProLong Gold antifade reagent with DAPI, Life Technologies) and examined by an Olympus BX41 fluorescent microscope. In some experiments, RAW-TLR9-HA cells transfected with mCAP18 plasmid or control plasmid were stimulated with 1uM CpG-C for 1 h. Cells were stained with anti-HA and anti-LAMP1.

In vivo experiments

For CpG-induced ear swelling, age and sex matched WT and *Camp*−/− mice were subcutaneously injected with 20 μg CpG-C in PBS into the left ear or PBS into the right ear. After 24 h, ear thickness was measured using a micrometer (Mitsutoyo). Ears from WT and *Camp*−/− mice were harvested 6 h after CpG-C injection for mRNA analyses. For *in vivo* CpG injection, WT and *Camp*−/− mice were administered 25 μg CpG-C intravenously. Serum was collected at 1 h for TNF-α and IL-6 detection and at 3h for IL-12p40 detection. For examining IFN-α production, 5 μg CpG was mixed with 20 μg DOTAP in HBS (Hepes-buffered saline: 20 mM HEPES, pH 7.4, containing 150 mM NaCl) according to the manufacturer's instructions. The mixture was administered intravenously (5 μg CpG-C in DOTAP / mouse). Serum was collected at 3 h for IFN-α detection.

Statistical analysis

Data are presented as mean ± SD. P-values were calculated with the two-tailed Student's t-test after the data were confirmed to fulfill the criteria.

Results

Camp−/− mice showed impaired CpG responses in vivo

To determine the physiological role of cathelicidin in recognition of CpG, WT and *Camp*−/− mice were administered CpG-C or LPS intravenously. *Camp*−/− mice showed lower amounts

of TNF-α, IL-6 and IL-12p40 production compared to WT controls after CpG-C injection, although the responses to LPS were comparable between WT and *Camp*$^{-/-}$ mice (Figure 1A–1D). We next intravenously injected a CpG-C/DOTAP complex into WT and in *Camp*$^{-/-}$ mice to initiate an IFN-α response (40) and observed a similar partial dependence on *Camp* expression (Figure 1E). Furthermore, *Camp*$^{-/-}$ mice showed reduced ear swelling after subcutaneous injection of CpG-C into the ears (Figure 1F). qPCR analysis of ear tissues after CpG-C injection demonstrated that *Camp*$^{-/-}$ mice also had reduced IL-6 and IL-12A induction but comparable level of TNF-α (Figure 1G). Taken together, these results indicated that cathelicidin enhances CpG responses *in vivo*. This effect did not appear to be due to an effect of cathelicidin on overall development of TLR or cytokine responses as the response to LPS was unaffected. This effect was consistent with prior observations that the human cathelicidin peptide LL-37 can influence the capacity of dendritic cells to recognize DNA (35).

Camp$^{-/-}$ DCs and macrophages show impaired CpG responses

To better understand how CpG recognition was influenced in *Camp*−/− mice we next studied the expression and function of the mouse cathelicidin (CRAMP) in dendritic cells derived from WT and *Camp*$^{-/-}$ mice. GM-CSF-induced BMDCs (GM-CSF BMDCs) abundantly expressed both full-length CRAMP protein and CRAMP peptide as seen by Western blotting (Figure 2A). We next prepared GM-CSF BMDCs from WT and *Camp*$^{-/-}$ mice under identical conditions. GM-CSF BMDCs derived from WT and *Camp*$^{-/-}$ mice had similar expression levels of MHC class II, costimulatory molecules, such as CD40, CD80 and CD86 and TLR9 (Supplemental Figure 1). Furthermore, WT and *Camp*$^{-/-}$ GM-CSF BMDCs exposed to LPS and ligands for TLR2, TLR3 and TLR7 had similar responses as measured by production of IL-6 and IL-12p40. However, similar to the decreased response seen *in vivo*, GM-CSF BMDCs derived from *Camp*$^{-/-}$ mice had a significantly impaired response to CpG-C (Figure 2B). A similar impaired response from *Camp*$^{-/-}$ GM-CSF BMDCs was seen to various other types of CpGs and at different concentration of the TLR9 ligand (Figure 2C–2E). GM-CSF BMDCs from *Camp*$^{-/-}$ mice on Balb/c background also showed impaired CpG-C responses but normal responses to LPS, indicating that the impaired CpG responses were not due to the strain specific artifacts (Figure 2F–2G). It is known that myeloid DCs produce IFN-β dependent on IRF-1 after TLR9 stimulation (41). *Camp*$^{-/-}$ GM-CSF BMDCs also produced less IFN-β (Supplemental Figure 2A). These results indicate that both NF-κB-dependent and IRF-1-dependent pathways are impaired in *Camp*$^{-/-}$ GM-CSF BMDCs.

Next, to examine the IRF-7 dependent IFN-α production in pDCs, we generated Flt3L-induced BMDCs (Flt3L BMDCs), which contains Flt3L pDCs and Flt3L cDCs. qPCR analysis showed that Flt3L BMDCs and thioglycollate-elicited peritoneal macrophages express *Camp* about 100 fold greater than that expressed by the keratinocyte cell line Pam212 (Figure 3A). We confirmed the expression of both full-length CRAMP protein and CRAMP peptide by Western blotting in Flt3L pDCs, Flt3L cDCs and peritoneal macrophages (Supplemental Figure 2B and data not shown). Similar to the observations in GM-CSF BMDCs, *Camp*$^{-/-}$ Flt3L pDCs showed reduced IFN-α, IL-6 and IL-12p40 production to CpG-A and CpG-C, indicating that the IRF-7 dependent pathway is also

affected (Figure 3B–3D and data not shown). *Camp*$^{-/-}$ Flt3L cDCs also showed impaired responses to CpG-C (Figure 3E). However, the responses to R848 and LPS were normal in *Camp*$^{-/-}$ Flt3L pDCs and Flt3L cDCs, respectively (Supplemental Figure 2C–2D). Furthermore, *Camp*$^{-/-}$ peritoneal macrophages showed impaired TNF-α and IL-6 production to CpG-C, although the responses to LPS were comparable between WT and *Camp*$^{-/-}$ peritoneal macrophages (Figure 3F–3G). These results indicate that endogenous cathelicidin affects CpG responses both in cultured cells and in primary cells.

Overexpression of mCAP18 enhances the TLR9 responses in RAW264.7 cells

To further examine the role of CRAMP in TLR9 responses, we generated RAW264.7 cells stably overexpressing mouse TLR9-HA (RAW-TLR9-HA cells). We overexpressed the full length cathelicidin mCAP18 plasmid or control plasmid in RAW-TLR9-HA cells. RAW-TLR9-HA cells transfected with control plasmid didn't express CRAMP, although RAW TLR9-HA cells overexpressing mCAP18 plasmid produced full-length CRAMP protein and processed it into the CRAMP peptide (Figure 4A). Overexpression of mCAP18 didn't affect the distribution of TLR9 which exists in the LAMP1 positive endolysosome after CpG stimulation (Figure 4B). In addition, the amount of full-length TLR9 and cleaved TLR9 was comparable after CpG stimulation between RAW-TLR9-HA cells transfected with mCAP18 plasmid and control plasmid (Figure 4C), indicating that CRAMP didn't have influence on the expression of TLR9. Consistent with the lesser response observed in *Camp*−/− mice, overexpression of mCAP18 enhanced responses to CpG-C, and the response to LPS was normal (Figure 4D). These results indicate that overexpression of mCAP18 enhances the CpG responses.

Endogenous cathelicidin facilitates signaling in GM-CSF BMDCs

To define the step at which endogenous cathelicidin works during CpG stimulation we next studied relative phosphorylation of downstream signaling intermediates. MAPKs and NF-κB signaling pathways are both involved in CpG-induced cytokine production (10). After CpG-B stimulation, *Camp*$^{-/-}$ GM-CSF BMDCs showed reduced phosphorylation and degradation of IκBα and reduced phosphorylation of MAPKs, such as ERK, JNK and p38 (Figure 5). These results were consistent with the diminished cytokine response and suggest that endogenous cathelicidin is important upstream from these signaling pathways.

Exogenous CRAMP failed to overcome the defects in Camp$^{-/-}$ BMDCs

We next sought to determine if endogenous expression of *Camp* influenced CpG uptake. WT and *Camp*$^{-/-}$ GM-CSF BMDCs were cultured with FITC-labelled CpG-C for 1 h. Analysis by flow cytometry demonstrated comparable CpG uptake between WT and *Camp*$^{-/-}$ GM-CSF BMDCs (Figure 6A). Normal endocytosis of CpG was further confirmed by immunofluorescence analysis (Figure 6B). These results suggested that CpG uptake is normal in *Camp*$^{-/-}$ GM-CSF BMDCs, although cytokine production from *Camp*$^{-/-}$ GM-CSF BMDCs was impaired (Figure 6C). To further determine if enhanced uptake could correct the cytokine response in *Camp*$^{-/-}$ GM-CSF BMDCs, we added the cationic transfection reagent DOTAP, a molecule that has been previously shown to enhance CpG uptake (42). Then, we stimulated WT and *Camp*$^{-/-}$ GM-CSF BMDCs with CpG-C or CpG-

C/DOTAP complex. DOTAP significantly increased CpG-induced cytokine production from both WT and *Camp*$^{-/-}$ GM-CSF BMDCs (Figure 6D). However, enhancing CpG entry did not overcome the defects in *Camp*$^{-/-}$ GM-CSF BMDCs. These results indicate that CpG uptake is not the reason for the difference in CpG responses between WT and *Camp*$^{-/-}$ GM-CSF BMDCs.

We next evaluated the effects of exogenous administration of mCRAMP on CpG-induced cytokine production. Previous reports have shown that the combination of LL-37 and DNA enhanced the TLR9 response (17). However, 10 μM mCRAMP, which is high concentration for *in vitro* experiments, had no influence on CpG uptake in BMDCs (Figure 7A). mCRAMP did increase the CpG response in WT GM-CSF BMDCs in a dose dependent manner, however, mCRAMP failed to rescue the defect in *Camp*$^{-/-}$ GM-CSF BMDCs (Figure 7B).

To examine whether BMDCs secrete CRAMP or another factor into the culture medium that could rescue the defect in *Camp*$^{-/-}$ BMDCs, WT GM-CSF BMDCs were cultured in complete medium for up to 24 hrs. Full-length CRAMP protein was observed to accumulate in this culture medium (Figure 7C). We then added WT and *Camp*$^{-/-}$ GM-CSF BMDCs to this conditioned medium and stimulated with CpG-C or R848. Conditioned media from WT BMDCs containing the CRAMP protein failed to rescue *Camp*$^{-/-}$ GM-CSF BMDCs (Figure 7D). In addition, the conditioned medium from WT BMDCs had no effect on CpG-induced and R848-induced cytokine production. These results indicate that the extracellular release of endogenous CRAMP is insufficient to overcome the defects in *Camp*$^{-/-}$.

CRAMP co-localized with CpG in the endolysosome and complexes with CpG and TLR9

BMDCs secreted full-length CRAMP protein into the culture medium, although they had more CRAMP peptide than full-length CRAMP protein in whole cell extracts (Figure 2A). In addition, exogenous CRAMP failed to rescue the defects in *Camp*$^{-/-}$ GM-CSF BMDCs. These results led us to hypothesize that intracellular CRAMP is involved in CpG responses. To explore the intracellular localization of CRAMP, Flt3L cDCs were stained with CRAMP and early endosomal marker, EEA1 or lysosomal marker, LAMP1. CRAMP colocalized with LAMP1 at steady state but not with EEA1 (Figure 8A-8B). After CpG-B stimulation for 90 min, CRAMP colocalized with LAMP1 and FITC-labelled CpG-B, indicating that CRAMP exists with CpG in the endolysosome where TLR9 binds to CpG after its cleavage (Figure 8B–8C).

We next examined whether CRAMP associates with TLR9. Co-immunoprecipitation experiments using RAW-TLR9-HA cells transfected with mCAP18 plasmid showed that TLR9 and CRAMP bind together even in the absence of CpG (Figure 9A–9B). LL-37 has a net positive charge and is known to bind to DNA. We next examined whether CRAMP binds to CpGs. mCRAMP was incubated with CpG-biotin and CpG-bound CRAMP was collected using streptavidin beads. CRAMP bound to various types of CpGs (Figure 9C). The amount of CRAMP that bound to CpG increased in a dose dependent manner (Figure 9D). Next we examined whether CRAMP peptide binds to TLR9 because only CRAMP peptide was seen after immunoprecipitation with anti-HA (Figure 9B). RAW-TLR9-HA cells were transfected with mCAP18 plasmid, CRAMP peptide plasmid or control plasmid.

Co-immunoprecipitation experiments showed that CRAMP peptide is sufficient to bind to TLR9 (Figure 9E–9F). Furthermore, in immunoprecipitation experiments with streptavidin, endogenous CRAMP peptide was seen only in WT GM-CSF BMDCs treated not with CpG-C but with CpG-C-biotin, indicating that CRAMP peptide binds to CpG intracellularly, suggesting that CRAMP may bind to CpG in endolysosome.

Discussion

In this report we identified a function for cathelicidin that has not been previously described but may play an important role in many of the infectious and inflammatory phenotypes associated with the expression of this gene. Our results suggest cathelicidin has an intracellular role in activation of TLR9 that acts independently of CpG uptake. This conclusion is based on observations that the absence of *Camp* decreased TLR9 responses *in vivo* and *in vitro* and that exogenous CRAMP did not increase CpG uptake. Furthermore, for the first time to our knowledge CRAMP was shown to be colocalized with CpG in the endolysosome and co-immunoprecipitated with CpG and TLR9. These findings reveal that cathelicidin is potentially an important intermediate for TLR9 action.

Cathelicidin has been shown to act by many different mechanisms to modulate immune responses. For example, one of the best described functions of cathelicidin is neutralization of LPS (28, 29). Both LL-37 and CRAMP have positive charge and will inhibit LPS by binding to it. Prior observations have shown that addition of micromolar quantities of extracellular recombinant cathelicidin, as well as other AMPs, will block the response to LPS in cultured cells (43). However, *Camp*$^{-/-}$ GM-CSF BMDCs do not show enhanced response to LPS when compared to WT GM-CSF BMDCs that abundantly expressed CRAMP within the cell. These findings suggest that GM-CSF BMDCs do not secrete enough CRAMP for neutralization of LPS, and that endogenous expression of cathelicidin does not have this function. Thus, observations from the experiments with recombinant cathelicidins can not be used to predict the activity of endogenously produced cathelicidin *in vivo*, and reflect more the pharmacologic potential of these peptides. The exact functions of intracellular cathelicidin produced under physiological conditions are not well understood.

In a screen to identify the physiologic function of cathelicidin endogenously expressed in mice, we did not detect a change in the response to the TLR7 ligand R848 but did observe a decrease in the response to the TLR9 ligand, CpG. TLR7 and TLR9 share similar signaling pathways (1). They exist in the ER and are delivered to the endosomes where they encounter and respond to their cognate antigens (44). After antigen recognition, they recruit MyD88 along with IRK4 and TRAF6, leading to NF-kB dependent inflammatory cytokine production (45). After CpG stimulation, endogenous cathelicidin affected the degradation of IκBα and phosphorylation of MAPKs and subsequent downstream signaling pathways, leading to IL-6, IL-12 and IFN-α production. Thus, these data imply that endogenous CRAMP works upstream from these signaling pathways and is specifically involved in TLR9 responses.

It has been previously shown that some cathelicidin peptides enhance the uptake of nucleotides into the cell (17, 31). LL-37 is able to form aggregates with self-DNA and self-

RNA. These aggregates are resistant to enzymatic degradation and can be delivered into human pDCs and human mDCs, leading to activation of TLR9 and TLR8, respectively. In addition, it has been shown that LL-37 and CpG complexes are efficiently transferred into human pDCs or B cells and facilitate their activation (35). However, CpG uptake in GM-CSF derived BMDCs was not decreased in cells from $Camp^{-/-}$ mice. We also found that even up to 10 μM mCRAMP did not alter CpG uptake. These results raised the question of why mCRAMP failed to enhance CpG uptake in contrast to LL-37 which does. This difference is likely due to the large difference in primary amino acid sequence between human LL-37 and mouse CRAMP (46). This difference may also be dependent on cell type. For example, in human cultured keratinocytes, premixed LL-37 and CpG complexes failed to enhance TLR9 responses (47). Overall these findings with the mature C-terminal cathelicidin peptides would predict that $Camp^{-/-}$ mice should not show a diminished response to CpG. Since we find that they do, this argues that the effects of cathelicidin in mice are independent of an extracellular effect of the mature peptide. Supporting this conclusion we also found that enhancing CpG uptake using CpG/DOTAP complexes failed to overcome defects the activation of $Camp^{-/-}$ BMDCs. $Camp^{-/-}$ mice also showed impaired IFN-α production after intravenous injection of CpG/DOTAP complexes.

TLR activation requires accessory molecules that are involved in ligand delivery and recognition, enzymatic cleavage of TLRs or trafficking of endosomal TLRs (48). Recently, HMGB1 and granulin were shown to also bind to CpG and help to deliver it into endosomes (13, 14, 16). Granulin directly also interacts with full length TLR9, although granulin is readily degraded by cathepsin which is important for TLR9 cleavage in endolysosome before ligand binding. Thus, after CpG delivery into endolysosomes, the existence of accessory molecules that affect TLR9 recognition and responses has precedence but is not well understood. Overexpression of mCAP18 didn't alter the distribution and cleavage of TLR9 or LPS responses but enhanced CpG responses. This also supports the importance of intracellular CRAMP. Our finding that CRAMP exists in endolysosome with CpG and binds intracellulary to TLR9 and CpG suggests that CRAMP might affect CpG recognition in the endolysosome. Due to technical issues and low transfection efficiency we were unable to determine if overexpression of CRAMP peptide alone enhanced the CpG response or if DCs derived from $Camp^{-/-}$ mice could be rescued by overexpression of cathelicidin. However, we could show that CRAMP peptide is sufficient for the binding between CRAMP and TLR9 and that overexpression of mCAP18 in RAW cell line that lacks CRAMP could enhance responses to CpG. Taken together with the lack of evidence of an extracellular effect that would be detected by a decrease in the LPS response, this supports the conclusion that intracellular cathelicidin acts as a TLR9 adapter molecule.

In conclusion, we show for the first time to our knowledge that endogenous intracellular cathelicidin is required for normal TLR9 function *in vitro* and *in vivo*. We hypothesize that cathelicidin can act in two ways to modify TLR9 activation. In humans, the mature cathelicidin peptide LL-37 can enhance nucleic acid uptake from the extracellular space (17, 31). However, CRAMP, the mouse ortholog of LL-37, does not have this function. In contrast, the presence of either mouse or human cathelicidin within the cell appears to bind both TLR9 and CpG. Our data support a model suggesting that this binding facilitates the

interaction between TLR9 and CpG to enhance release of cytokines and interferon alpha. This agrees with clinical associations of increased inflammation seen in conditions of enhanced cathelicidin expression and the prevailing theory that cathelicidin has important consequences for host defense and autoimmunity in disorders such as psoriasis and rosacea. The present findings therefore provide new insight into the function of cathelicidin.

Supplementary Material

Refer to Web version on PubMed Central for supplementary material.

References

1. Kawai T, Akira S. Toll-like receptors and their crosstalk with other innate receptors in infection and immunity. Immunity. 2011; 34:637–650. [PubMed: 21616434]

2. Akira S, Uematsu S, Takeuchi O. Pathogen recognition and innate immunity. Cell. 2006; 124:783–801. [PubMed: 16497588]

3. Takeuchi O, Akira S. Pattern recognition receptors and inflammation. Cell. 2010; 140:805–820. [PubMed: 20303872]

4. Chen GY, Nunez G. Sterile inflammation: sensing and reacting to damage. Nat Rev Immunol. 2010; 10:826–837. [PubMed: 21088683]

5. Kumagai Y, Takeuchi O, Akira S. TLR9 as a key receptor for the recognition of DNA. Adv Drug Deliv Rev. 2008; 60:795–804. [PubMed: 18262306]

6. Ewald SE, Lee BL, Lau L, Wickliffe KE, Shi GP, Chapman HA, Barton GM. The ectodomain of Toll-like receptor 9 is cleaved to generate a functional receptor. Nature. 2008; 456:658–662. [PubMed: 18820679]

7. Park B, Brinkmann MM, Spooner E, Lee CC, Kim YM, Ploegh HL. Proteolytic cleavage in an endolysosomal compartment is required for activation of Toll-like receptor 9. Nat Immunol. 2008; 9:1407–1414. [PubMed: 18931679]

8. Ewald SE, Engel A, Lee J, Wang M, Bogyo M, Barton GM. Nucleic acid recognition by Toll-like receptors is coupled to stepwise processing by cathepsins and asparagine endopeptidase. J Exp Med. 2011; 208:643–651. [PubMed: 21402738]

9. Sepulveda FE, Maschalidi S, Colisson R, Heslop L, Ghirelli C, Sakka E, Lennon-Dumenil AM, Amigorena S, Cabanie L, Manoury B. Critical role for asparagine endopeptidase in endocytic Toll-like receptor signaling in dendritic cells. Immunity. 2009; 31:737–748. [PubMed: 19879164]

10. Kawai T, Akira S. The role of pattern-recognition receptors in innate immunity: update on Toll-like receptors. Nat Immunol. 2010; 11:373–384. [PubMed: 20404851]

11. Honda K, Yanai H, Negishi H, Asagiri M, Sato M, Mizutani T, Shimada N, Ohba Y, Takaoka A, Yoshida N, Taniguchi T. IRF-7 is the master regulator of type-I interferon-dependent immune responses. Nature. 2005; 434:772–777. [PubMed: 15800576]

12. Sasai M, Linehan MM, Iwasaki A. Bifurcation of Toll-like receptor 9 signaling by adaptor protein 3. Science. 2010; 329:1530–1534. [PubMed: 20847273]

13. Ivanov S, Dragoi AM, Wang X, Dallacosta C, Louten J, Musco G, Sitia G, Yap GS, Wan Y, Biron CA, Bianchi ME, Wang H, Chu WM. A novel role for HMGB1 in TLR9-mediated inflammatory responses to CpG-DNA. Blood. 2007; 110:1970–1981. [PubMed: 17548579]

14. Tian J, Avalos AM, Mao SY, Chen B, Senthil K, Wu H, Parroche P, Drabic S, Golenbock D, Sirois C, Hua J, An LL, Audoly L, La Rosa G, Bierhaus A, Naworth P, Marshak-Rothstein A, Crow MK, Fitzgerald KA, Latz E, Kiener PA, Coyle AJ. Toll-like receptor 9-dependent activation by DNA-containing immune complexes is mediated by HMGB1 and RAGE. Nat Immunol. 2007; 8:487–496. [PubMed: 17417641]

15. Yanai H, Ban T, Wang Z, Choi MK, Kawamura T, Negishi H, Nakasato M, Lu Y, Hangai S, Koshiba R, Savitsky D, Ronfani L, Akira S, Bianchi ME, Honda K, Tamura T, Kodama T, Taniguchi T. HMGB proteins function as universal sentinels for nucleic-acid-mediated innate immune responses. Nature. 2009; 462:99–103. [PubMed: 19890330]

16. Park B, Buti L, Lee S, Matsuwaki T, Spooner E, Brinkmann MM, Nishihara M, Ploegh HL. Granulin is a soluble cofactor for toll-like receptor 9 signaling. Immunity. 2011; 34:505–513. [PubMed: 21497117]

17. Lande R, Gregorio J, Facchinetti V, Chatterjee B, Wang YH, Homey B, Cao W, Su B, Nestle FO, Zal T, Mellman I, Schroder JM, Liu YJ, Gilliet M. Plasmacytoid dendritic cells sense self-DNA coupled with antimicrobial peptide. Nature. 2007; 449:564–569. [PubMed: 17873860]

18. Nakatsuji T, Gallo RL. Antimicrobial peptides: old molecules with new ideas. J Invest Dermatol. 2012; 132:887–895. [PubMed: 22158560]

19. Braff MH, Bardan A, Nizet V, Gallo RL. Cutaneous defense mechanisms by antimicrobial peptides. J Invest Dermatol. 2005; 125:9–13. [PubMed: 15982297]

20. Nizet V, Ohtake T, Lauth X, Trowbridge J, Rudisill J, Dorschner RA, Pestonjamasp V, Piraino J, Huttner K, Gallo RL. Innate antimicrobial peptide protects the skin from invasive bacterial infection. Nature. 2001; 414:454–457. [PubMed: 11719807]

21. Iimura M, Gallo RL, Hase K, Miyamoto Y, Eckmann L, Kagnoff MF. Cathelicidin mediates innate intestinal defense against colonization with epithelial adherent bacterial pathogens. J Immunol. 2005; 174:4901–4907. [PubMed: 15814717]

22. Chromek M, Slamova Z, Bergman P, Kovacs L, Podracka L, Ehren I, Hokfelt T, Gudmundsson GH, Gallo RL, Agerberth B, Brauner A. The antimicrobial peptide cathelicidin protects the urinary tract against invasive bacterial infection. Nat Med. 2006; 12:636–641. [PubMed: 16751768]

23. Barlow PG, Svoboda P, Mackellar A, Nash AA, York IA, Pohl J, Davidson DJ, Donis RO. Antiviral activity and increased host defense against influenza infection elicited by the human cathelicidin LL-37. PLoS One. 2011; 6:e25333. [PubMed: 22031815]

24. Howell MD, Jones JF, Kisich KO, Streib JE, Gallo RL, Leung DY. Selective killing of vaccinia virus by LL-37: implications for eczema vaccinatum. J Immunol. 2004; 172:1763–1767. [PubMed: 14734759]

25. De Y, Chen Q, Schmidt AP, Anderson GM, Wang JM, Wooters J, Oppenheim JJ, Chertov O. LL-37, the neutrophil granule- and epithelial cell-derived cathelicidin, utilizes formyl peptide receptor-like 1 (FPRL1) as a receptor to chemoattract human peripheral blood neutrophils, monocytes, and T cells. J Exp Med. 2000; 192:1069–1074. [PubMed: 11015447]

26. Tjabringa GS, Aarbiou J, Ninaber DK, Drijfhout JW, Sorensen OE, Borregaard N, Rabe KF, Hiemstra PS. The antimicrobial peptide LL-37 activates innate immunity at the airway epithelial surface by transactivation of the epidermal growth factor receptor. J Immunol. 2003; 171:6690–6696. [PubMed: 14662872]

27. Elssner A, Duncan M, Gavrilin M, Wewers MD. A novel P2X7 receptor activator, the human cathelicidin-derived peptide LL37, induces IL-1 beta processing and release. J Immunol. 2004; 172:4987–4994. [PubMed: 15067080]

28. Mookherjee N, Brown KL, Bowdish DM, Doria S, Falsafi R, Hokamp K, Roche FM, Mu R, Doho GH, Pistolic J, Powers JP, Bryan J, Brinkman FS, Hancock RE. Modulation of the TLR-mediated inflammatory response by the endogenous human host defense peptide LL-37. J Immunol. 2006; 176:2455–2464. [PubMed: 16456005]

29. Di Nardo A, Braff MH, Taylor KR, Na C, Granstein RD, McInturff JE, Krutzik S, Modlin RL, Gallo RL. Cathelicidin antimicrobial peptides block dendritic cell TLR4 activation and allergic contact sensitization. J Immunol. 2007; 178:1829–1834. [PubMed: 17237433]

30. Kahlenberg JM, Kaplan MJ. Little peptide, big effects: the role of LL-37 in inflammation and autoimmune disease. J Immunol. 2013; 191:4895–4901. [PubMed: 24185823]

31. Ganguly D, Chamilos G, Lande R, Gregorio J, Meller S, Facchinetti V, Homey B, Barrat FJ, Zal T, Gilliet M. Self-RNA-antimicrobial peptide complexes activate human dendritic cells through TLR7 and TLR8. J Exp Med. 2009; 206:1983–1994. [PubMed: 19703986]

32. Lai Y, Adhikarakunnathu S, Bhardwaj K, Ranjith-Kumar CT, Wen Y, Jordan JL, Wu LH, Dragnea B, San Mateo L, Kao CC. LL37 and cationic peptides enhance TLR3 signaling by viral double-stranded RNAs. PLoS One. 2011; 6:e26632. [PubMed: 22039520]

33. Hasan M, Ruksznis C, Wang Y, Leifer CA. Antimicrobial peptides inhibit polyinosinic-polycytidylic acid-induced immune responses. J Immunol. 2011; 187:5653–5659. [PubMed: 22048772]

34. Singh D, Qi R, Jordan JL, San Mateo L, Kao CC. The human antimicrobial peptide LL-37, but not the mouse ortholog, mCRAMP, can stimulate signaling by poly(I:C) through a FPRL1-dependent pathway. J Biol Chem. 2013; 288:8258–8268. [PubMed: 23386607]

35. Hurtado P, Peh CA. LL-37 promotes rapid sensing of CpG oligodeoxynucleotides by B lymphocytes and plasmacytoid dendritic cells. J Immunol. 2010; 184:1425–1435. [PubMed: 20042575]

36. Ong PY, Ohtake T, Brandt C, Strickland I, Boguniewicz M, Ganz T, Gallo RL, Leung DY. Endogenous antimicrobial peptides and skin infections in atopic dermatitis. N Engl J Med. 2002; 347:1151–1160. [PubMed: 12374875]

37. Yamasaki K, Di Nardo A, Bardan A, Murakami M, Ohtake T, Coda A, Dorschner RA, Bonnart C, Descargues P, Hovnanian A, Morhenn VB, Gallo RL. Increased serine protease activity and cathelicidin promotes skin inflammation in rosacea. Nat Med. 2007; 13:975–980. [PubMed: 17676051]

38. Di Nardo A, Vitiello A, Gallo RL. Cutting edge: mast cell antimicrobial activity is mediated by expression of cathelicidin antimicrobial peptide. J Immunol. 2003; 170:2274–2278. [PubMed: 12594247]

39. Nakagawa Y, Takamatsu H, Okuno T, Kang S, Nojima S, Kimura T, Kataoka TR, Ikawa M, Toyofuku T, Katayama I, Kumanogoh A. Identification of semaphorin 4B as a negative regulator of basophil-mediated immune responses. J Immunol. 2011; 186:2881–2888. [PubMed: 21270411]

40. Blasius AL, Arnold CN, Georgel P, Rutschmann S, Xia Y, Lin P, Ross C, Li X, Smart NG, Beutler B. Slc15a4, AP-3, and Hermansky-Pudlak syndrome proteins are required for Toll-like receptor signaling in plasmacytoid dendritic cells. Proc Natl Acad Sci U S A. 2010; 107:19973–19978. [PubMed: 21045126]

41. Schmitz F, Heit A, Guggemoos S, Krug A, Mages J, Schiemann M, Adler H, Drexler I, Haas T, Lang R, Wagner H. Interferon-regulatory-factor 1 controls Toll-like receptor 9-mediated IFN-beta production in myeloid dendritic cells. Eur J Immunol. 2007; 37:315–327. [PubMed: 17273999]

42. Yasuda K, Yu P, Kirschning CJ, Schlatter B, Schmitz F, Heit A, Bauer S, Hochrein H, Wagner H. Endosomal translocation of vertebrate DNA activates dendritic cells via TLR9-dependent and -independent pathways. J Immunol. 2005; 174:6129–6136. [PubMed: 15879108]

43. Rosenfeld Y, Papo N, Shai Y. Endotoxin (lipopolysaccharide) neutralization by innate immunity host-defense peptides. Peptide properties and plausible modes of action. J Biol Chem. 2006; 281:1636–1643. [PubMed: 16293630]

44. Latz E, Schoenemeyer A, Visintin A, Fitzgerald KA, Monks BG, Knetter CF, Lien E, Nilsen NJ, Espevik T, Golenbock DT. TLR9 signals after translocating from the ER to CpG DNA in the lysosome. Nat Immunol. 2004; 5:190–198. [PubMed: 14716310]

45. Ishii KJ, Akira S. Innate immune recognition of, and regulation by, DNA. Trends Immunol. 2006; 27:525–532. [PubMed: 16979939]

46. Pestonjamasp VK, Huttner KH, Gallo RL. Processing site and gene structure for the murine antimicrobial peptide CRAMP. Peptides. 2001; 22:1643–1650. [PubMed: 11587792]

47. Morizane S, Yamasaki K, Muhleisen B, Kotol PF, Murakami M, Aoyama Y, Iwatsuki K, Hata T, Gallo RL. Cathelicidin antimicrobial peptide LL-37 in psoriasis enables keratinocyte reactivity against TLR9 ligands. J Invest Dermatol. 2012; 132:135–143. [PubMed: 21850017]

48. Lee CC, Avalos AM, Ploegh HL. Accessory molecules for Toll-like receptors and their function. Nat Rev Immunol. 2012; 12:168–179. [PubMed: 22301850]
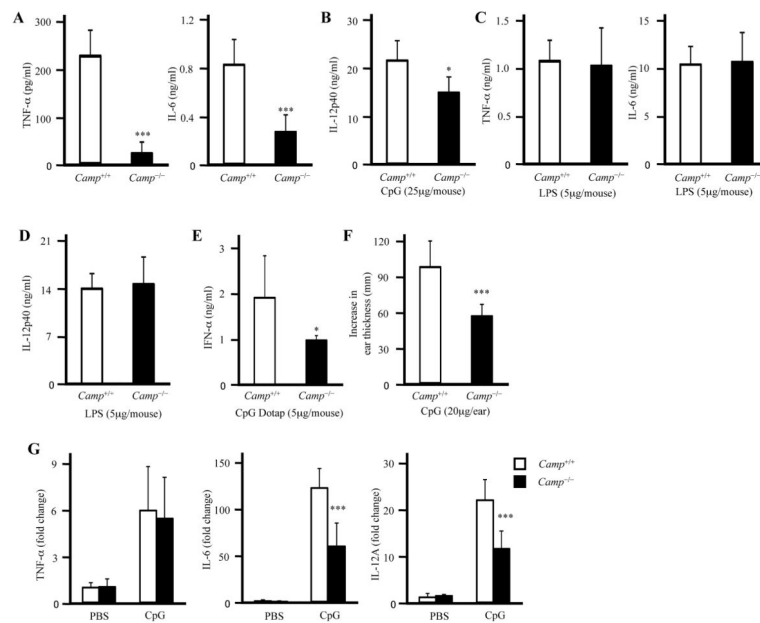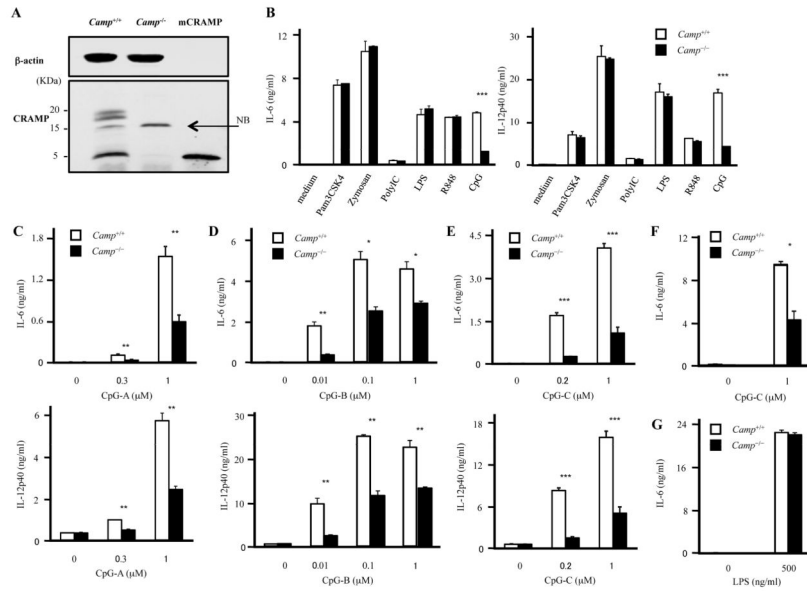
Figure 1. *Camp*$^{-/-}$ **mice show impaired CpG response** *in vivo*
A and B, WT and *Camp*$^{-/-}$ mice were injected with 25 μg CpG-C (A and B) or 5 μg LPS (C and D) intravenously. Serum was collected 1 h (A and C) and 3 h (B and D) after CpG-C or LPS injection and the cytokine concentration in the serum was measured by ELISA (n = 7). E, WT and *Camp*$^{-/-}$ mice were injected with 5 μg CpG-C/DOTAP complex intravenously. Serum was collected 3 h after CpG-C/DOTAP complex injection and IFN-α concentration in the serum was measured by ELISA (n=7). F and G, WT and *Camp*$^{-/-}$ mice were injected PBS or 20 μg CpG-C into the ears subcutaneously. The increase in the ear thickness 24 h after injection was measured (n = 9) (F). Q-PCR data of the ear skin 6 h after injection (n = 6) (G).
*P < 0.05, ***P < 0.005. Data were representative of three independent experiments.

Figure 2. GM-CSF- BMDCs from *Camp*^{−/−} mice show impaired CpG responses
A, GM-CSF- BMDCs express both full-length CRAMP protein and CRAMP peptide by
Western blotting. Cell lysates from WT and *Camp*^{−/−} GM-CSF BMDCs were prepared and
similar amounts of protein lysates were immunoblotted using Abs against CRAMP and β-
actin. Synthetic mCRAMP peptide was used for positive control. NB: non-specific band B,
WT and *Camp*^{−/−} BMDCs were stimulated with Pam3CSK4 (1 μg/ml), Zymozan (10 μg/
ml), PolyIC (10 μg/ml), LPS (500 ng/ml), R848 (0.2 μg/ml) and CpG-C (1 μM) for 15 h.
The cytokine concentration in the supernatants was measured by ELISA. C, D and E, WT
and *Camp*^{−/−} GM-CSF BMDCs were stimulated with various concentration of CpG-A (C),
CpG-B (D) and CpG-C (E) for 15 h. The cytokine concentration in the supernatants was
measured by ELISA. F and G, GM-CSF BMDCs derived from WT and *Camp*^{−/−} mice in a
Balb/c background were stimulated with CpG-C (F) and LPS for 15 h. The cytokine
concentration in the supernatants was measured by ELISA.
*P < 0.05, **P < 0.01 ***P < 0.005. Data are representative of at least three independent
experiments.
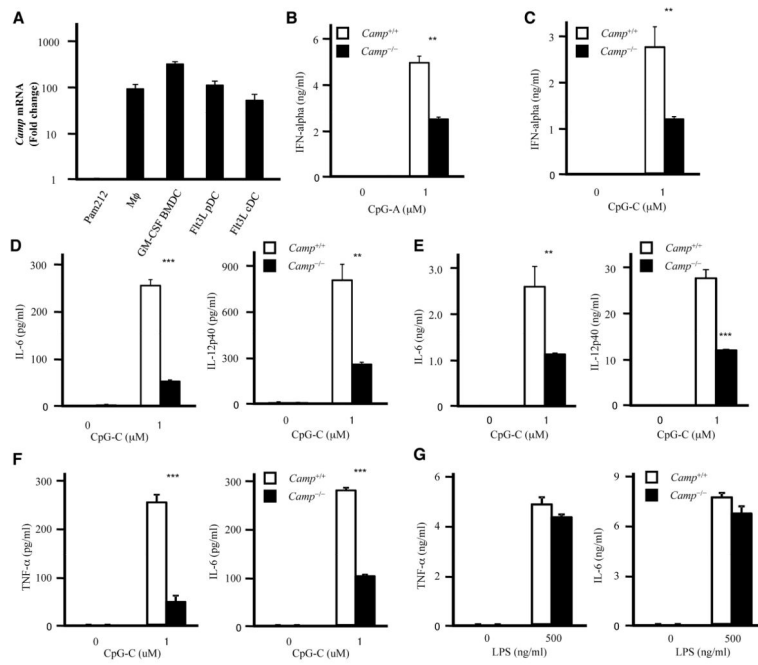
Figure 3. Impaired CpG responses in _Camp^−/−_ macrophages and dendritic cells
A, _Camp_ mRNA expression in macrophages and dendritic cells. Real-time PCR was used to quantify mRNA levels and fold change values are calculated relative to and normalized to _Gapdh_ expression for _Camp_. Mφ: thioglycollate-elicited peritoneal macrophage. B and C, Flt3L pDCs were stimulated with CpG-A (B) or CpG-C (C) for 15 h. IFN-α in the culture supernatants was measured by ELISA. D and E, Flt3L pDCs (D) or Flt3L cDCs (E) were stimulated with CpG-C for 15 h. The cytokine concentration in the supernatants was measured by ELISA. F and G, Thioglycollate-elicited peritoneal macrophages from WT and _Camp^−/−_ mice were stimulated with CpG-C (F) or LPS (G) for 15 h. The cytokine concentration in the supernatants was measured by ELISA.
**P < 0.01 ***P < 0.005. Data are representative of at least three independent experiments.
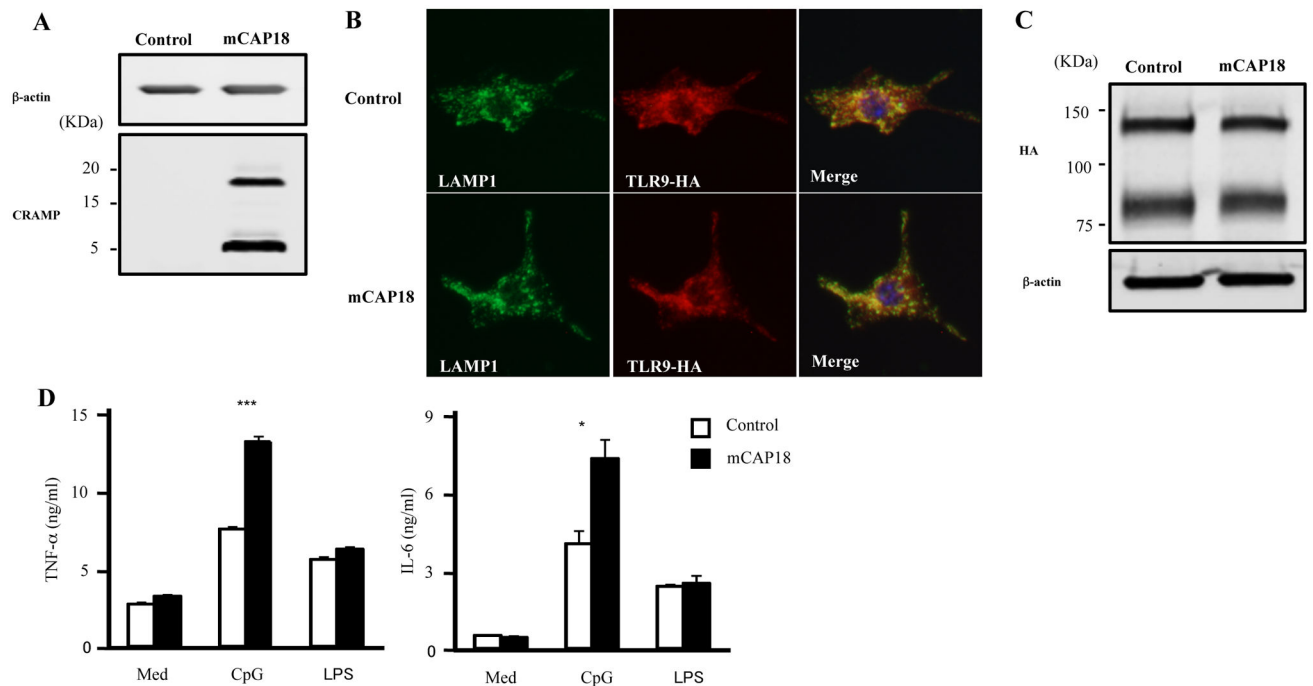
Figure 4. Overexpression of mCAP18 enhances TLR9 response
A, CRAMP expression in RAW-TLR9-HA cells which were transiently transfected with plasmid encoding the full length mouse cathelicidin precursor protein (mCAP18) or control plasmid (control) was analyzed by Western blotting. B and C, RAW-TLR9-HA cells were transiently transfected with mCAP18 or control. Cells were stimulated with 1 μM CpG-C for 1 h. Cells were permeabilized and stained for HA (Alexa 568; red) and LAMP1 (Alexa 488; green). Nuclei were stained with DAPI (blue) (B). Cells were lysed and TLR9-HA expression was analyzed by Western blotting (C) D, RAW-TLR9-HA cells were transiently transfected with pSELECT-puro-mCAP18 or pSELECT-puro-mcs. Cells were stimulated with CpG-C (0.2 μM) and LPS (500 ng/ml) for 15 h. The cytokine concentration in the supernatants was measured by ELISA. Data are representative of three independent experiments.
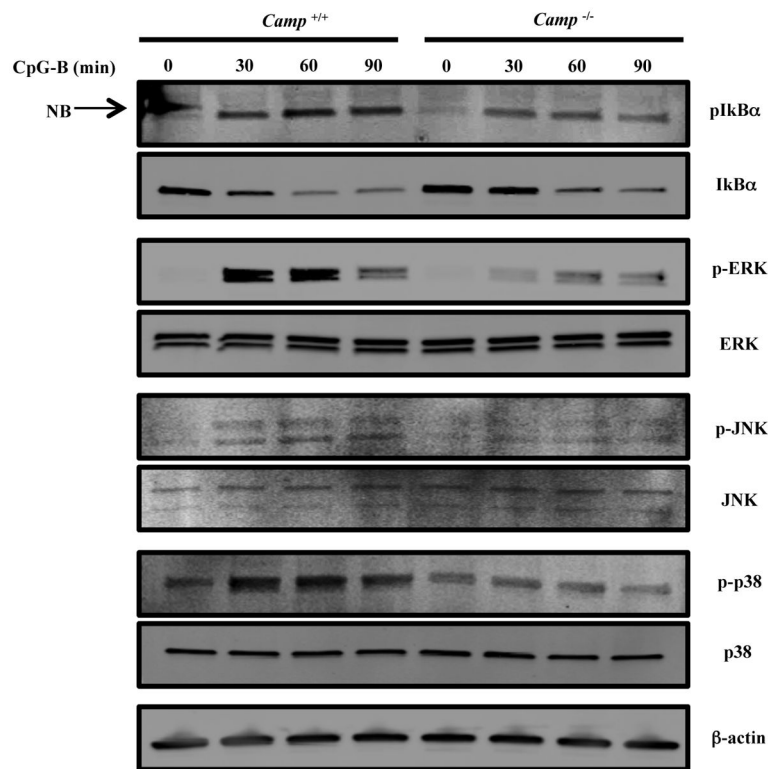
Figure 5. *Camp* is required for the activation of TLR9 signaling pathway
WT and *Camp*$^{-/-}$ GM-CSF BMDCs were stimulated with 1 μM CpG-B. Cell lysates were prepared at the indicated times. Protein extracts were immunoblotted using Abs against phospho-IκBα, ERK, JNK or p-38 and total IκBα, ERK, JNK, p-38 or β-actin. NB: non-specific band. Data are representative of three independent experiments.
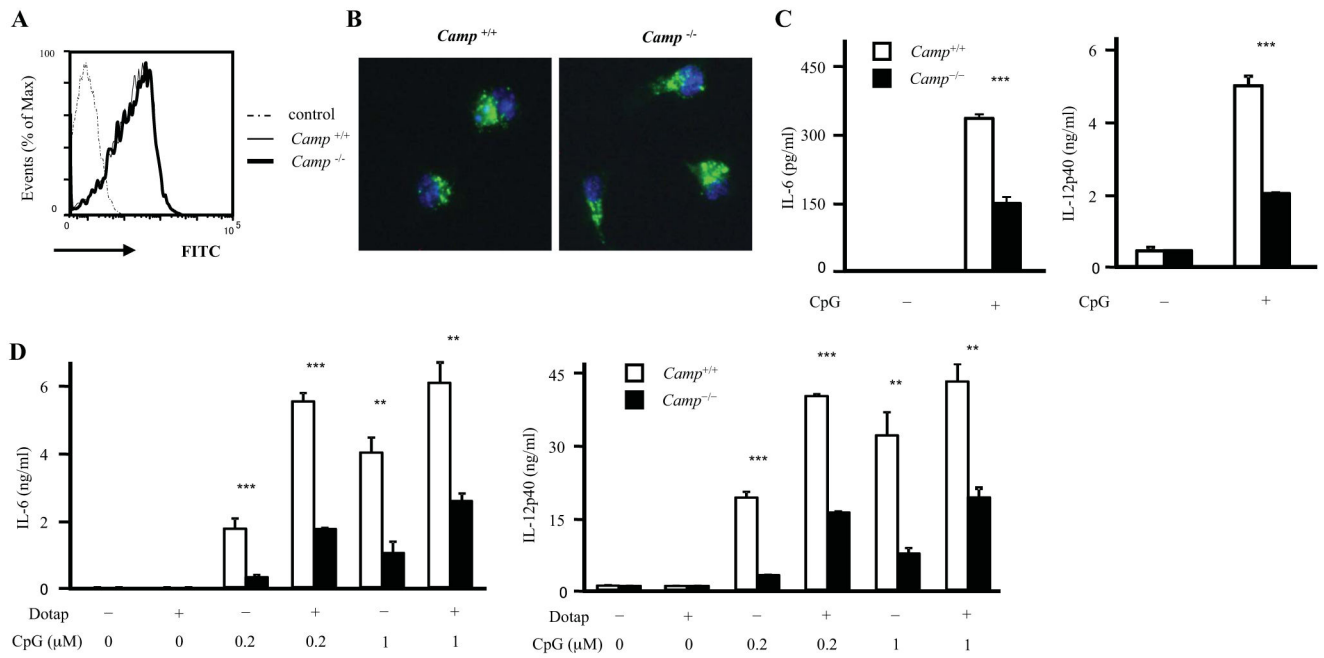
Figure 6. CpG uptake is normal in *Camp*$^{-/-}$ BMDCs

A and B, *Camp*$^{-/-}$ GM-CSF BMDCs show normal CpG uptake. WT and *Camp*$^{-/-}$ GM-CSF BMDCs were cultured with 1 μM FITC-labelled CpG-C for 1 h. Cells were washed and analyzed by flow cytometery (A). Cells were fixed with 4% formaldehyde for 5 min, stained with DAPI and analyzed by fluorescence microscopy (B). C, WT and *Camp*$^{-/-}$ GM-CSF BMDCs were cultured with 1 μM FITC-labelled CpG-C for 1 h. Cells were washed and same numbers of cells in complete medium were plated in 96-well plates and cultured for 15 h. The supernatants were measured by ELISA (C). D, WT and *Camp*$^{-/-}$ GM-CSF BMDCs were stimulated with various concentration of CpG-C or CpG-C/DOTAP complex for 15 h. The supernatants were measured by ELISA.

$**P < 0.01$ $***P < 0.005$. Data are representative of three independent experiments.
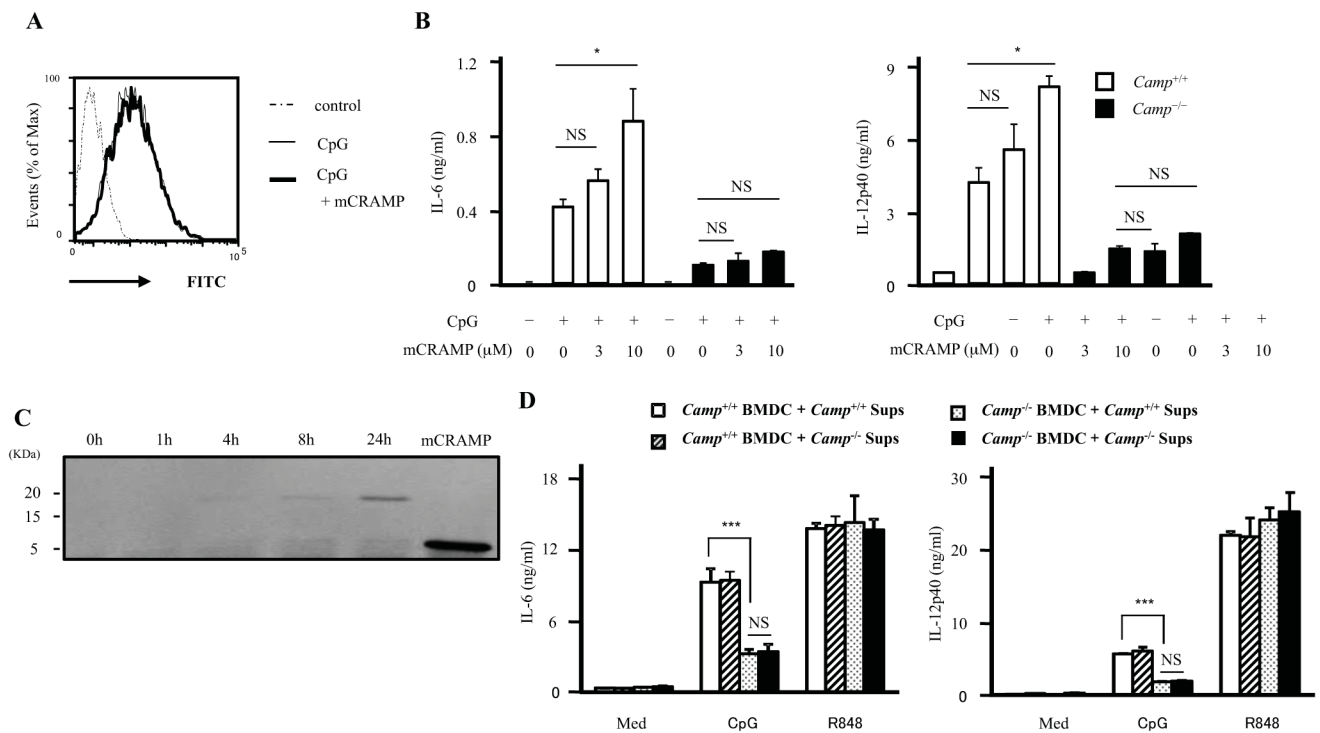
Figure 7. Exogenous CRAMP fails to rescue impaired CpG responses in *Camp*$^{-/-}$ BMDCs
A, WT GM-CSF BMDCs were cultured with 1uM FITC-labelled CpG-C for 1 h in the presence or absence of 10 μM mCRAMP. Cells were washed and analyzed by flow cytometery. B, WT and *Camp*$^{-/-}$ GM-CSF BMDCs were stimulated with 0.2 μM CpG-C in the presence of various concentration of mCRAMP. The supernatants were measured by ELISA. C, WT GM-CSF BMDCs (3×107 cells/ml) were cultured in the complete medium. The conditioned medium was collected at the indicated time. Equal volumes of conditioned medium and mCRAMP for positive control were immunoblotted with anti-CRAMP Ab. D, WT and *Camp*$^{-/-}$ GM-CSF BMDCs were cultured for 24 h and the conditioned medium was collected (*Camp*$^{+/+}$ sups or *Camp*$^{-/-}$ sups). WT and *Camp*$^{-/-}$ GM-CSF BMDCs were stimulated with CpG-C (1 μM) and R848 (0.2 μg/ml) in *Camp*$^{+/+}$ sups or *Camp*$^{-/-}$ sups for 15 h. The supernatants were measured by ELISA.
**P < 0.01 ***P < 0.005. Data are representative of three independent experiments.
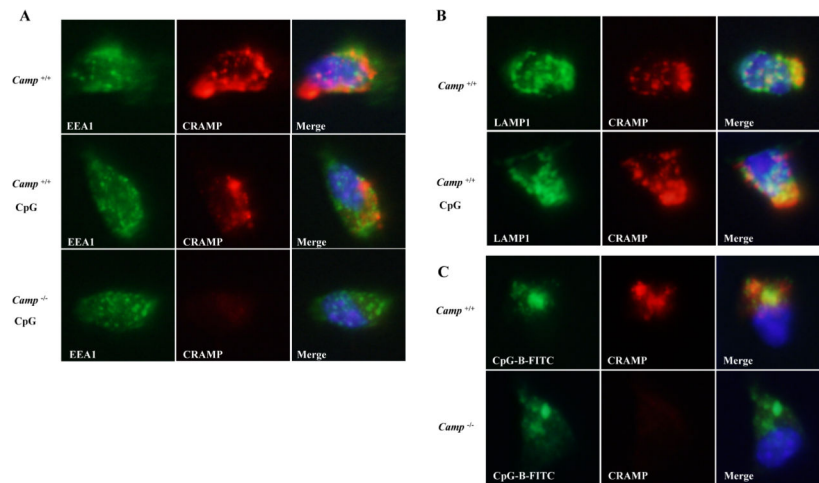
Figure 8. CRAMP colocalizes with CpG in the endolysosome and associates with TLR9
A, WT and *Camp*$^{-/-}$ Flt3L cDCs were stimulated with or without 1 μM CpG-B for 90 min. Cells were fixed, permeabilized and stained for CRAMP (Alexa 568; red) and EEA1 (Alexa 488; green, A). Nuclei were stained with DAPI (blue). The localization of CRAMP was analyzed by fluorescence microscopy. B, WT Flt3L cDCs were stimulated with or without 1 μM CpG-B for 90 min. Cells were fixed, permeabilized and stained for CRAMP (Alexa 568; red) and LAMP1 (Alexa 488; green, B). C, WT and *Camp*$^{-/-}$ Flt3L cDCs were stimulated with 1 μM FITC-labelled CpG-B for 90 min. Cells were fixed and stained for CRAMP (Alexa 568; red).
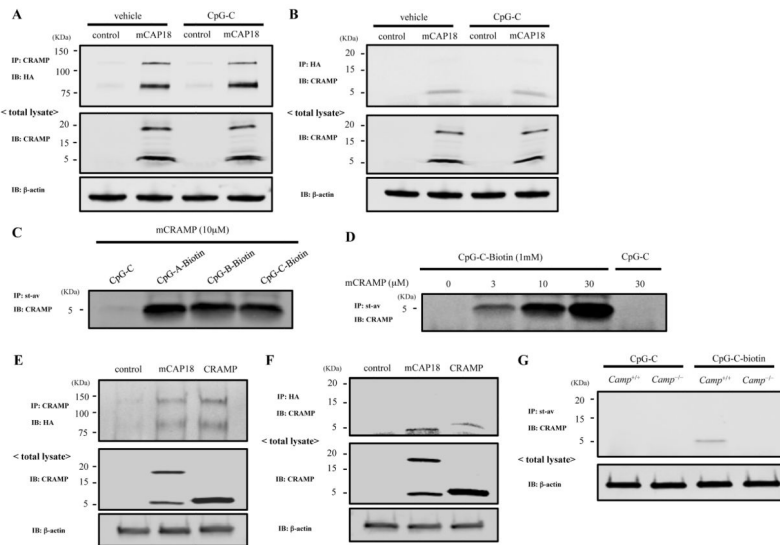
Figure 9. CRAMP binds to CpG DNA
A and B, RAW-TLR9-HA cells transfected with mCAP18 or control were stimulated with or without 1 μM CpG-C for 90 min. Cells were washed and lysed. Cell lysates were immunoprecipitated with anti-CRAMP and immunoblotted with anti-HA (A) or immunoprecipitated with anti-HA and immunoblotted with anti-CRAMP (B). Total cell lysates were immunoblotted with anti-CRAMP or β-actin for control. C, 10 μM mCRAMP was incubated with 1 μM CpG-C or 1 μM biotinylated-CpG-A, -CpG-B or -CpG-C for 1 h. Biotinylated-CpG was recovered by streptavidin beads, and then binding of CRAMP to CpG was examined by immunoblot with anti-CRAMP. D, Various concentration of mCRAMP were incubated with 1 μM CpG-C or 1 μM biotinylated-CpG-C for 1 h. Biotinylated-CpG was recovered by streptavidin beads, and then binding of CRAMP to CpG was examined by immunoblot with anti-CRAMP. E and F, RAW-TLR9-HA cells were transfected with mCAP18, CRAMP or control. Cells were lysed and immunoprecipitated with anti-CRAMP and immunoblotted with anti-HA, or immunoprecipitated with anti-HA and immunoblotted with anti-CRAMP. G, WT and *Camp*$^{-/-}$ GM-CSF BMDCs were stimulated with 1 μM CpG-C or CpG-C-biotin for 1 h. Cells were washed and lysed. Cell lysates were incubated with streptavidin beads. CpG-C-biotin-bound CRAMP was immunoblotted with anti-CRAMP. Data are representative of three independent experiments.